DOI: 10.1002/cssc.201100782

Tuning the Acid/Metal Balance of Carbon Nanofiber-Supported Nickel Catalysts for Hydrolytic Hydrogenation of Cellulose

Stijn Van de Vyver,[a] Jan Geboers,[a] Wouter Schutyser,[a] Michiel Dusselier,[a] Pierre Eloy,[b] Emmie Dornez,[c] Jin Won Seo,[d] Christophe M. Courtin,[c] Eric M. Gaigneaux,[b] Pierre A. Jacobs,[a] and Bert F. Sels*[a]

Carbon nanofibers (CNFs) are a class of graphitic support materials with considerable potential for catalytic conversion of biomass. Earlier, we demonstrated the hydrolytic hydrogenation of cellulose over reshaped nickel particles attached at the tip of CNFs. The aim of this follow-up study was to find a relationship between the acid/metal balance of the Ni/CNFs and their performance in the catalytic conversion of cellulose. After oxidation and incipient wetness impregnation with Ni, the Ni/CNFs were characterized by various analytical methods. To prepare a selective Ni/CNF catalyst, the influences of the nature of oxidation agent, Ni activation, and Ni loading were investigated. Under the applied reaction conditions, the best result, that is, 76% yield in hexitols with 69% sorbitol selectivity at 93% conversion of cellulose, was obtained on a 7.5 wt% Ni/CNF catalyst prepared by chemical vapor deposition of CH_4 on a Ni/γ-Al_2O_3 catalyst, followed by oxidation in HNO_3 (twice for 1 h at 383 K), incipient wetness impregnation, and reduction at 773 K under H_2. This preparation method leads to a properly balanced Ni/CNF catalyst in terms of Ni dispersion and hydrogenation capacity on the one hand, and the number of acidic surface-oxygen groups responsible for the acid-catalyzed hydrolysis on the other.

Introduction

In the framework of carbohydrate-based biorefinery schemes, the search for catalytic processes for converting cellulose has been intense.[1] A particularly promising reaction in water is the one-pot hydrolytic hydrogenation of cellulose to sugar alcohols. Although discovered decades ago,[2] this chemistry was recently reinvestigated for a wide range of heterogeneous catalysts. Among the screened candidates are supported noble-metal catalysts, such as Pt/γ-Al_2O_3,[3] Pt/carbon black,[4] Pt/H-ZSM-5,[5] Pt/MCM-48,[6] Ru/activated carbon,[7] Ru/C,[8] or Pt catalysts[9] in combination with heteropolyacids (HPAs), Ru/H-USY zeolites with trace amounts of HCl,[10] Ru/CNTs,[11] Ru/$Cs_3PW_{12}O_{40}$,[12] [RuCl(CO)H(PPh_3)$_3$]/KOH in 1-butyl-3-methylimidazolium,[13] RhNi/MC,[14] and combinations of Pt/C, Pd/C, or Ru/C with dilute HCl,[15] H_3PO_4, or H_2SO_4.[16] Catalytic hydrogenolysis of cellulose to ethylene glycol by using Ni-W_2C/AC,[17] Ni-W/SBA-15,[18] WC_x supported on mesoporous carbon,[19] or Ru/C in the presence of WO_3[20] has been studied as well.

In 2010, two groups reported almost simultaneously the use of nickel as a less expensive alternative metal catalyst for the transformation of cellulose into C_6 sugar alcohols.[1a] Ding et al. focused on a bifunctional nickel phosphide catalyst (16% Ni_2P/AC), yielding up to 48% sorbitol under optimized reaction conditions (498 K, 6 MPa H_2 added at RT).[21] Mechanistically, hydrolysis of cellulose into glucose is proposed to be catalyzed by the acidity formed by excess phosphide, followed by nickel-catalyzed hydrogenation of glucose to sorbitol. In parallel, we investigated the catalytic conversion of cellulose over as-synthesized carbon nanofibers (CNFs) with nickel particles at the tip of the fibers.[22] When compared with conventional carbon materials, aggregates of CNFs present interesting properties, such as enhanced mechanical strength and filterability, high hydrothermal stability, controllable surface chemistry, and reduced mass transfer limitations associated with the presence of mesopores and a high surface area.[23] The combination of these features makes them suitable candidates for applications as catalyst supports in biomass-related reactions. Accordingly, when using as-prepared CNF-supported nickel catalysts (Ni/CNFs) for the conversion of cellulose, yields of sorbitol in the range of 30–50% were obtained under mild reaction condi-

[a] Dr. S. Van de Vyver, Dr. J. Geboers, W. Schutyser, M. Dusselier, Prof. Dr. P. A. Jacobs, Prof. Dr. B. F. Sels
Centre for Surface Chemistry and Catalysis
Katholieke Universiteit Leuven
Kasteelpark Arenberg 23, 3001 Heverlee (Belgium)
Fax: (+32) 1632-1998
E-mail: bert.sels@biw.kuleuven.be

[b] P. Eloy, Prof. Dr. E. M. Gaigneaux
Unité de catalyse et chimie des matériaux divisés
Université catholique de Louvain
Croix du Sud, 2/17B-1348 Louvain-la-Neuve (Belgium)

[c] Dr. E. Dornez, Prof. Dr. C. M. Courtin
Laboratory of Food Chemistry and Biochemistry
Katholieke Universiteit Leuven
Kasteelpark Arenberg 20, 3001 Heverlee (Belgium)

[d] Prof. Dr. J. W. Seo
Department of Metallurgy and Materials Engineering
Katholieke Universiteit Leuven
Kasteelpark Arenberg 44, 3001 Heverlee (Belgium)

 © 2012 Wiley-VCH Verlag GmbH & Co. KGaA, Weinheim

tions (463–503 K, 6 MPa H_2 added at RT).[22] While this method gave moderate sugar alcohol yields for a non-noble-metal catalyst, we noted that the preparation of the Ni/CNF catalyst could be targeted for further optimization.

Numerous articles have appeared on the synthesis[24] and use of Ni/CNFs in catalytic reactions such as methane decomposition;[25] liquid-phase hydrogenation of benzene;[26] and gas-phase hydrogenations of crotonaldehyde,[27] butyronitrile,[28] nitrobenzene,[29] ethylene,[30] 1-butene, and 1,3-butadiene.[30a,31] Different methods for supporting metal particles on CNFs have been reviewed as well.[32] In the case of Ni, routinely applied methodologies include incipient wetness impregnation,[26,27,30–31,33] ion-exchange,[34] electroless plating,[35] and deposition/precipitation.[28,29,33,36] The anchoring and dispersion of Ni precursors on inert CNFs can be achieved by the introduction of oxygen-containing surface groups using treatment with oxidizing gases (e.g., O_2, N_2O, CO_2) or aqueous solutions of oxidizing acids such as HNO_3, H_2SO_4, or H_2O_2.[24a,37] It is assumed that this type of oxidation starts with the formation of phenolic and carbonyl groups at the sp^2-hybridized, edge-site carbon atoms on the CNF surface.[38] Upon continuing oxidation, the groups are converted into carboxylic acid and anhydride groups.

Herein, we focus on the use of CNFs grown by chemical vapor deposition (CVD) as a support material, using a standard incipient wetness impregnation technique for the deposition of Ni. Compared with our previously reported catalyst based on Ni nanoclusters partially embedded in graphene layers,[22] oxidative activation of the CNFs is not only performed for effectively anchoring more and well-dispersed Ni particles,[39] it also opens perspectives on tailoring the acid strength/concentration for improved catalytic activity during the hydrolytic hydrogenation of cellulose.

Results and Discussion

Preparation and characterization of Ni/CNFs

Catalytic CVD of methane over a 20 wt% Ni/γ-Al_2O_3 catalyst, calcined and reduced at 873 K, results in CNFs of the fishbone type with the graphene layers inclined with respect to the central fiber axis.[22] From N_2 physisorption isotherms, a relatively large and accessible surface area of 102 $m^2 g^{-1}$ was found with a total pore volume of 0.16 $cm^3 g^{-1}$ and a micropore volume of 0.01 $cm^3 g^{-1}$. A combined SEM and Raman spectroscopy study showed an average fiber diameter of 60 nm with an in-plane crystallite size of 21 nm. More detailed morphological and structural characteristics of the CNFs have been previously published.[22]

To introduce different amounts of acidic groups and anchoring sites for the Ni particles, the CNFs were heated at reflux once or twice for 1 h in either concentrated HNO_3 or 1:1 mixtures of HNO_3/H_2SO_4. The methodology is based on previous reports,[38b,40] which documented the influence of both oxidation agents on the texture of fishbone-type CNFs and the number of oxygen-containing surface groups. Herein, acid–base titration of the CNF suspensions in water, NH_3 temperature-programmed desorption (NH_3-TPD), and temperature-programmed decomposition were used to investigate the amount, strength, and stability of the acidic groups. The results (Table 1), in correlation with the catalytic behavior of the Ni/CNFs, are discussed in the next sections. Regarding the effect of oxidation on the textural properties, three representative N_2 physisorption isotherms of the untreated, the HNO_3-, and the HNO_3/H_2SO_4-oxidized CNFs are shown in Figure 1a. The presence of hysteresis loops is attributed to the condensation of N_2 between the open spaces of the entangled CNFs at high relative pressure.[41] While the observed increase in mesopore volume indicates a less dense macrostructure, Ros et al. previously associated the larger surface area to an altered surface roughness of the oxidized CNF surface.[38b]

Nickel was deposited on the oxidized CNFs by incipient wetness impregnation with an aqueous solution of nickel nitrate, followed by drying and reduction under a flow of H_2. To find balanced acid and hydrogenation activity of the catalysts, the influence of metal loading was investigated by using different concentrations of the Ni precursor ($[Ni^{2+}] = 0.17$–0.95 mmol L^{-1}). As measured by ICP-AES, the actual Ni loadings of the resulting Ni/CNFs varied from 2.6 to 10.4 wt%. The dispersion of the Ni particles was determined by using pulse CO

Table 1. Acid treatment method, nominal and actual Ni loading, reduction temperature, physicochemical features, Ni dispersion, and amount of Ni surface atoms of various Ni/CNF catalysts.

Entry	Acid treatment	Ni uptake[a] [wt%]	Ni loading[b] [wt%]	Reduction T [K]	S_{BET} [$m^2 g^{-1}$]	Pore V [$cm^3 g^{-1}$]	Acid density[c] [mmol g^{-1}]	Ni dispersion[d] [%]	Ni surface atoms[e] [μmol $g_{cat.}^{-1}$]
1	1×1 h HNO_3/H_2SO_4	6	8.4	773	146	0.37	0.00 (0.20)	0.5	6.5
2	2×1 h HNO_3/H_2SO_4	6	7.8	773	154	0.44	0.00 (0.32)	0.6	7.3
3	1×1 h HNO_3	6	7.5	773	137	0.33	0.02 (0.06)	1.8	23.3
4	2×1 h HNO_3	6	7.6	773	139	0.36	0.03 (0.07)	2.2	28.2
5	2×1 h HNO_3	3	2.9	573	118	0.25	0.12	3.6	17.7
6	2×1 h HNO_3	3	3.2	673	130	0.27	0.10	2.9	15.7
7	2×1 h HNO_3	3	3.9	773	132	0.29	0.02	1.9	12.7
8	2×1 h HNO_3	3	5.6	873	138	0.31	<0.01	1.2	11.6
9	2×1 h HNO_3	3	7.3	973	128	0.33	<0.01	0.5	6.6

[a] Nominal Ni loading on the CNF support. [b] Quantitative elemental analysis of the actual Ni loading performed by inductively coupled plasma atomic emission spectroscopy (ICP-AES). [c] Determined by acid–base titrations. Values in parentheses refer to the corresponding acid densities of the unloaded CNFs after oxidation treatment. [d] Calculated from the actual Ni loading and the amount of Ni surface atoms. [e] Determined by pulsed CO titration experiments.

 © 2012 Wiley-VCH Verlag GmbH & Co. KGaA, Weinheim

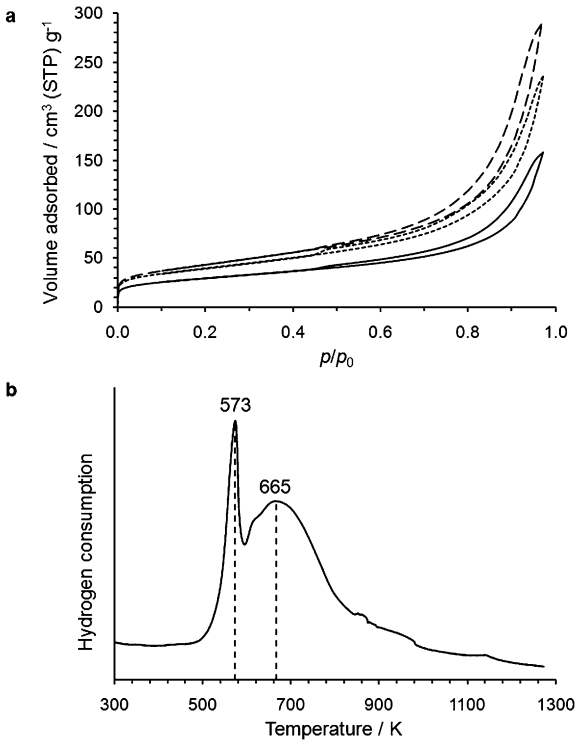

Figure 1. a) N_2 physisorption isotherms at 77 K of the parent CNFs grown by CVD of methane over a Ni/γ-Al_2O_3 catalyst (——) and after oxidation in either HNO_3 (-----) or a 1:1 mixture of HNO_3/H_2SO_4 (– – –). The isotherms can be classified as type IV isotherms with type B hysteresis loops. b) H_2-TPR profile of the catalysts precursor after deposition of Ni onto the HNO_3-treated CNF support by incipient wetness impregnation and subsequent drying in air.

chemisorption measurements (Table 1) and TEM. Figure 2 shows an example of a TEM micrograph of a 7.5 wt% Ni/CNF catalyst, indicating a rather broad distribution of the Ni particle sizes centered around 16 nm. The impregnation and subsequent reduction of oxidized CNFs yield Ni dispersions ranging from 0.5 to 3.6%. For the Ni/CNF catalysts, the amount of accessible Ni surface atoms is listed in Table 1.

The reduction behavior of the Ni/CNFs was studied by H_2 temperature-programmed reduction (H_2-TPR) of the catalyst precursor after deposition of the Ni compound onto the CNF support (Figure 1b). When using a heating rate of 10 K min^{-1}, the reduction peaks were found at 573 and 665 K. In line with previous work,[29,36b,42] the two stages of H_2 consumption are ascribed to the reduction of the Ni precursor and catalytic gasification of the CNFs, respectively. The latter phenomenon is characterized by a significant weight loss of the CNFs, explaining the discrepancy between the nominal and actual Ni loading of the samples reduced at temperatures above 773 K (Table 1). MS monitoring of the gas stream evolved during the H_2-TPR experiments showed the initial formation of methane at temperatures around 523 K. This implies the availability of metallic Ni, which is indispensable in providing active hydrogen for gasification of the CNFs.[41] In our systematic study of preparation conditions, the initially chosen temperature of 773 K was suitable to ensure the reduction of the Ni/CNF catalyst, while limiting the extent of CNF gasification.

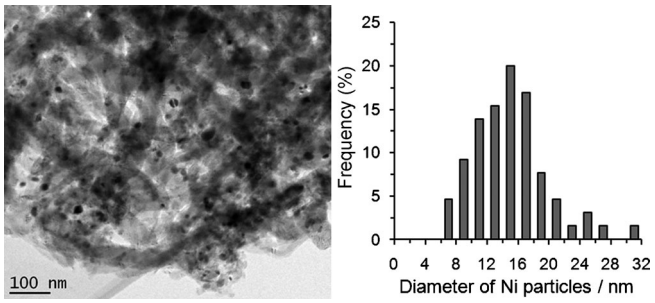

Figure 2. TEM micrograph and the corresponding histogram of the Ni particle size distribution of a 7.5 wt% Ni/CNFs catalyst prepared by impregnation of $Ni(NO_3)_2 \cdot 6H_2O$ onto HNO_3-oxidized CNFs followed by H_2 reduction at 773 K.

Typical product spectrum

The hydrolytic hydrogenation of cellulose with Ni/CNFs was studied at 463 K and 6 MPa H_2 added at RT (see the Experimental Section). Prior to the catalytic reactions, the reactivity of Avicel cellulose towards dissolution and catalytic hydrolysis was enhanced by ball-milling.[1,22] Detailed characterization data (such as SEM, XRD, ^{13}C cross polarization magic angle spinning (CP-MAS) NMR spectroscopy, and FTIR spectroscopy) of the ball-milled cellulose samples have been provided elsewhere.[22,43]

Figure 3 shows the cellulose conversion changes in time over an optimized 7.5 wt% Ni/CNF catalyst, prepared by the liquid-phase oxidation of the CNFs in HNO_3, incipient wetness impregnation, and reduction at 773 K. At 93% cellulose conversion, yields of 64% sorbitol and 7% mannitol were obtained, which are significantly higher than those previously reported under identical conditions for untreated CNFs with Ni particles at the tip of the fibers (50% sorbitol and 5% mannitol at 92% conversion).[20]

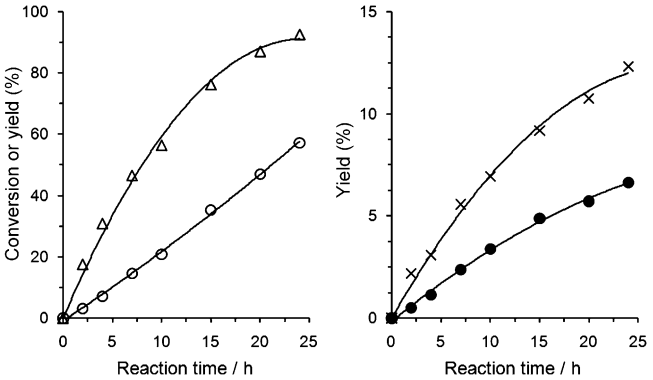

Figure 3. Changes with time of the conversion of cellulose (△) and yields of sorbitol (○), erythritol (×), and mannitol (●). Reaction conditions: ball-milled Avicel cellulose (1 g), water (50 mL), 6 MPa initial H_2 pressure at RT, 463 K, 24 h, with 7.5 wt% Ni/CNF catalyst (0.5 g) prepared by oxidation (twice in HNO_3 for 1 h), followed by incipient wetness impregnation and reduction at 773 K.

 © 2012 Wiley-VCH Verlag GmbH & Co. KGaA, Weinheim

Generally, the experimental sorbitol/mannitol product ratio ranged from 5 to 10. Whereas sorbitol and mannitol are known to be produced through the hydrogenation of glucose and mannose, the literature attributes the formation of mannose to the acid-catalyzed C2 epimerization of glucose.[1v] Although not always mentioned,[1b] a multitude of byproducts can be formed during the metal-catalyzed cracking of cellulose. For example, in the presence of the 7.5 wt% Ni/CNF catalyst, we identified small amounts of 1,4-sorbitan (3.6%), glycerol (3.5%), 1,2-butanediol (2.8%), xylitol (1.8%), and trace amounts (< 1%) of 1,2-propanediol, isosorbide, 1,2-hexanediol, and ethylene glycol. The dehydration of sorbitol to isosorbide follows an intramolecular dehydration step to generate 1,4-sorbitan intermediates and subsequent dehydration to isosorbide.[44] On the other hand, ethylene glycol, glycerol, 1,2-propanediol, and other low-molecular-weight polyols were earlier shown to originate from metal-catalyzed hydrogenolysis.[17] While the carbon balance in the liquid phase accounted for more than 90% of the initial number of carbon atoms, it is interesting to note that a product analysis of the gaseous effluent showed only small amounts of CH_4 (0.3%) and CO_2 (0.1%). The remaining gap in the carbon balance should be attributed to the formation of water-soluble cello-oligomers.[45]

Effect of the nature of the oxidation agent for support treatment

The most important characteristics of the four catalyst samples used in this section are given in entries 1–4 of Table 1. Prior to Ni deposition, CNFs were oxidized by heating at reflux once or twice for 1 h in either concentrated HNO_3 or 1:1 (*v*/*v*) mixtures of HNO_3/H_2SO_4. The results from acid–base titrations, denoted in parentheses in Table 1, demonstrate that the number of acidic sites on the surface of the CNFs depends on both the oxidation agent and the treatment time. It has been shown elsewhere that the concentration of nitronium ions (i.e., the active nitrating species) is higher for HNO_3/H_2SO_4 mixtures [Reaction (1)] than for concentrated HNO_3 [Reaction (2)].[40,46]

$$HNO_3 + 2\,H_2SO_4 \rightleftharpoons NO_2^+ + HSO_4^- + H_3O^+ \quad (1)$$

$$2\,HNO_3 \rightleftharpoons NO_2^+ + NO_3^- + H_2O \quad (2)$$

Indeed, results from X-ray photoelectron spectroscopy (XPS) analyses given in Table 2 show a much higher O 1s/C 1s peak area ratio when the CNFs were treated in HNO_3/H_2SO_4 mixtures. Deconvolution of the O 1s region resulted in about 4–5% oxygen-containing species with a binding energy (E_b) of 535.1 eV, which could be assigned to carboxylic acids.[47]

After impregnation with Ni, CO chemisorption results indicate that, for an identical reduction temperature (773 K), the oxidation agent has a pronounced effect on the dispersion of the Ni particles. Using only HNO_3, Ni dispersions of about 2% could be obtained, while with HNO_3/H_2SO_4-treated CNFs, the dispersion values were consistently lower (Table 1). Because the HNO_3/H_2SO_4-treated CNFs seem to have lost all of the acidic groups, the impact of impregnation and reduction of the Ni/CNFs requires some clarification. The higher agglomeration degree of Ni on the HNO_3/H_2SO_4-treated CNFs is correlated to the decomposition of less stable surface oxygen groups during the reduction stage, which facilitates the mobility and agglomeration of the Ni particles on the CNF surface.[41] This effect was observed in the XPS spectra by a strong decrease of the O 1s/C 1s peak area ratio from 0.122 to 0.043 after reduction of the Ni/CNFs. A similar conclusion was drawn in studies by Calvillo et al. on the preparation of Pt/CNFs with HNO_3 and HNO_3/H_2SO_4 mixtures.[48]

Table 2. XPS results of the O/C ratio and relative contents of the O 1s groups for CNFs treated twice for 1 h in HNO_3/H_2SO_4 or in concentrated HNO_3.[a]

Oxidation agent	O/C	Fraction of each O 1s component [%]				
		Peak 1	Peak 2	Peak 3	Peak 4	Peak 5
HNO_3/H_2SO_4	0.122	31.9	19.2	41.3	3.8	3.8
HNO_3	0.065	20.9	25.4	42.6	4.6	6.5

[a] Deconvolution of the O 1s region:[47] peak 1 (531.4 eV), peak 2 (532.6 eV), peak 3 (533.5 eV), peak 4 (535.1 eV), and peak 5 (536.7 eV).

As seen in Figure 4, the investigated oxidation variables significantly influence the overall conversion of cellulose and selectivity towards the products formed in the hydrolytic hydrogenation reaction. For the sake of clarity, only the amounts of sorbitol, mannitol, erythritol, and C_2–C_5 hydrogenolysis products are plotted. At first glance, HNO_3 is more suitable as an oxidation agent for the preparation of Ni/CNFs, resulting in enhanced yields of sorbitol and mannitol. In case of HNO_3/H_2SO_4-treated CNFs, the lower hexitol selectivities are partly due to strong sintering of Ni particles, which reduces the active metal surface for catalytic hydrogenation of the released glucose. However, only a different hydrogenation activity cannot adequately explain the observed differences in product selectivity and cellulose conversion. In Figure 4, the considerable difference between the conversion of cellulose, as measured by

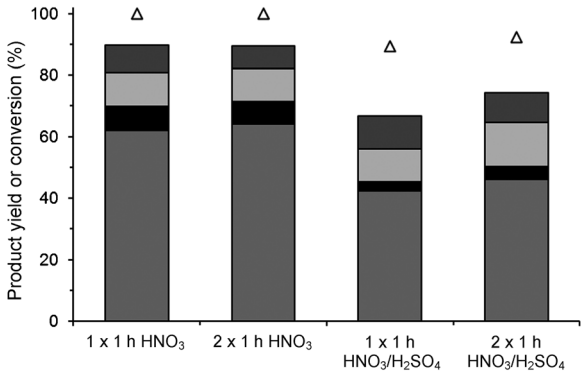

Figure 4. Comparison of the conversion and product yields of different Ni/CNF catalysts for the hydrolytic hydrogenation of cellulose (■ sorbitol, ■ mannitol, ■ erythritol, ■ C_2–C_5 products, △ conversion). Reaction conditions: ball-milled Avicel cellulose (1 g), Ni/CNF catalyst (0.5 g), water (50 mL), 6 MPa initial H_2 pressure at RT, 463 K, 24 h.

 © 2012 Wiley-VCH Verlag GmbH & Co. KGaA, Weinheim

total organic carbon (TOC) analysis of the aqueous phase, and the sum of chromatographically identified products suggests significant changes in the formation of cello-oligomers, depending on the oxidation agent.

Differences are even more compelling among the chromatograms shown in Figure 5, representing relative amounts of β-1,4-glucan fragments determined after 24 h of reaction by using high-performance anion-exchange chromatography with pulsed amperometric detection (HPAEC-PAD; see the Experimental Section). Recently,[10] the dissolution–conversion of ball-milled Avicel cellulose in water at 463 K and 5 MPa H_2 has been demonstrated to generate up to 80% cello-oligomers even in the absence of any catalyst. From Figure 5 it is clear

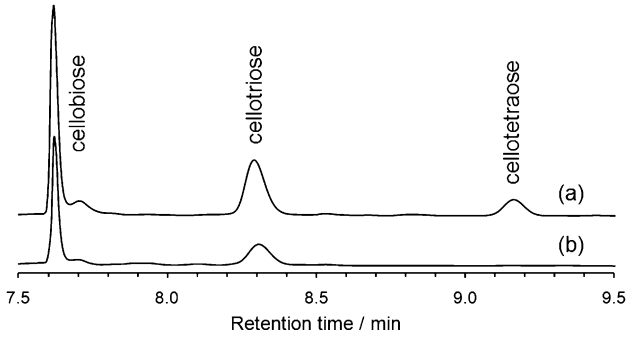

Figure 5. HPAEC-PAD analysis of the water-soluble cello-oligomer fragments released during the reaction of ball-milled cellulose with Ni/CNFS pretreated with a) 2×1 h 1:1 (v/v) mixtures of HNO_3/H_2SO_4 or b) 2×1 h concentrated HNO_3.

that the reaction of cellulose with nonacidic Ni/CNFs results in a more than twofold greater β-1,4-glucan formation than acidic compounds. In qualitative terms, hydrolysis of the cello-oligomers to glucose seems to be the rate-determining step when using nonacidic Ni/CNF catalysts. However, by introducing small amounts of thermally stable Brønsted acid sites (i.e., up to 0.03 mmol H^+ per g of catalyst) through pre-oxidation of the CNFs with HNO_3, the reaction rates for hydrolysis of β-1,4-glucans to glucose are observed to be much higher, thereby yielding significantly less cello-oligomers and more hexitols in the product spectrum (Figure 4 vs. Figure 5).

Effect of catalyst reduction temperature

Having identified HNO_3 as the most effective oxidation agent, we examined the effect of reduction temperature on the properties and catalytic activity of the Ni/CNFs. From entries 5–9 in Table 1, it can be derived that, while the specific surface area and pore volume remain approximately constant, the dispersion of the Ni particles decreases significantly with increasing reduction temperature. After 1 h reduction at 973 K (heating rate 5 K min^{-1}), the Ni dispersion calculated from CO chemisorption even drops to 0.5% (Table 1, entry 9). The sintering process of carbon-supported Ni particles during a reduction treatment has long been recognized.[49] Studies by Baker have shown a relationship between the mobility of Ni particles on a graphite surface and the Tamman temperature of the metal.[49a] In the current investigation, it can be speculated that the reasons for the relatively high susceptibility to Ni agglomeration/growth are related to the weak interaction of the Ni precursor with the CNF support,[36b] as well as to the higher actual temperature at the CNF surface due to the heat released by catalytic gasification.[41]

As reported above, heat treatment of the Ni/CNFs under a reducing atmosphere also leads to the removal of the oxygen-containing surface groups. In Table 1, a clear trend can be observed in the decrease of acid density of the Ni/CNFs with increasing reduction temperature. After reduction at 573 K, the acid density of the catalyst amounted to 0.12 mmol H^+ per g, while for the samples reduced at 873 and 973 K less than 0.01 mmol g^{-1} of residual Brønsted acidity remained. The loss of acidity from the Ni/CNFs was confirmed by ammonia temperature-programmed desorption (NH_3-TPD) after NH_3 adsorption at 473 K (Figure 6). Regardless of the low signal-to-noise ratio, it is clear that the amount of NH_3 desorbed from the Ni/CNFs has significantly decreased after reduction at higher temperatures. The NH_3-TPD profile associated with the sample reduced at 773 K reveals the presence of two desorption peaks. While the low-temperature peak centered at 400 K arises from weakly held NH_3 molecules (probably hydrogen bonded), the broad signal in the temperature range between 420 and 800 K is assigned to the presence of stronger Brønsted acid sites.

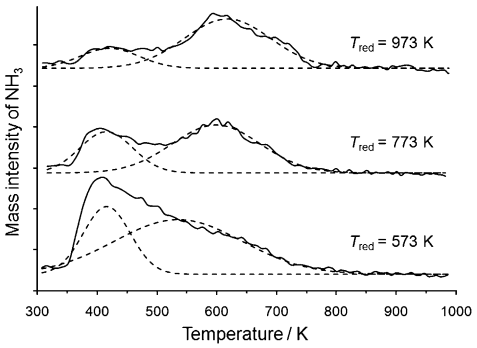

Figure 6. TPD profiles of NH_3 adsorbed at 473 K from Ni/CNFs pretreated at different reduction temperatures. The dashed lines under the curves represent a best fit for a two-peak profile assuming Gaussian distribution.

To unravel the nature of the surface oxygen complexes responsible for this acidity, the functionalized Ni/CNFs were further investigated by temperature-programmed decomposition in He with simultaneous analysis of CO and CO_2 evolution (Figure 7). The literature available on chemical activation of carbon materials reports seven possible types of oxygen-containing groups on the surface of CNFs (i.e., carboxylic acids, lactones, phenols, carbonyls, ethers, carboxylic anhydrides, and quinone groups).[38b] In general, the most acidic groups are thermally transformed into CO_2, whereas less acidic and more stable ones decompose into CO.[50] Although there is no general consensus on the assignment of the peaks in Figure 7 to specific functionalities, the profiles indicate a drastic decrease

 © 2012 Wiley-VCH Verlag GmbH & Co. KGaA, Weinheim

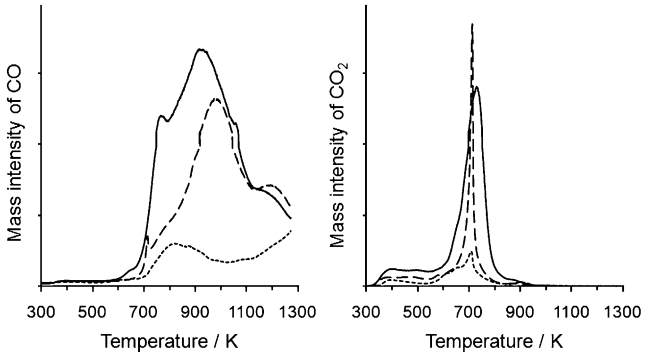

Figure 7. CO and CO_2 evolution during temperature-programmed decomposition of the Ni/CNFs samples pretreated at different reduction temperatures (—— 573, – – – 773, and ----- 973 K). Ordinate: relative signal intensities at *m/z* 28 for CO (left) and 44 for CO_2 (right).

Table 3. Effect of the reduction temperature of the Ni/CNF catalysts on the conversion of cellulose and product yields.[a]

Reduction temperature [K]	Conversion [%]	Yield [%] hexitols	sorbitol	C_2–C_5 products
573	82.0	32.4	23.9	28.5
673	88.0	45.9	35.4	26.4
773	90.6	58.0	47.6	25.8
873	88.0	43.8	35.1	26.4
973	86.9	41.6	33.3	33.0

[a] Reaction conditions: ball-milled Avicel cellulose (1 g), Ni/CNF catalyst (0.5 g), water (50 mL), 6 MPa initial H_2 pressure at RT, 463 K, 24 h.

in the number of surface groups with increasing reduction temperature. From the results in Figure 7 and in agreement with earlier work,[40,51] we conclude that only few acidic surface groups remain upon treatment of the Ni/CNFs at 973 K. It should be noted that the sample reduced at 973 K still gives desorption of CO and CO_2 at temperatures below 973 K, diagnostic of the formation of surface-oxygen complexes upon air exposure during catalyst handling after the reduction step.[52]

From the results given in Table 3, a maximum in the catalytic activity is found for the Ni/CNFs reduced at 773 K, with a cellulose conversion reaching 91% and a hexitol yield of 58%. For reduction temperatures going from 553 to 773 K, the enhancement in hexitol formation indicates an improved balance between the acid and hydrogenation functions (see below). Based on the XPS spectra of these materials, it is instructive to note that the ratio of Ni^0 species (E_b = 852.6 eV) to Ni^{2+} (E_b = 854.6) increases from 8:92 to 19:81 after reduction at 553 and 773 K, respectively.[53] However, although the ratio further increases to 24:76 for Ni/CNFs activated at 973 K, the observed yield to hexitols drops to 42%. This trend can be explained by the lower dispersion of the bigger Ni particles hampering efficient participation in the hydrogenation and by the lack of hydrolytic activity on the CNF surface with an acid density below 0.01 mmol H^+ per g.

Effect of Ni loading

In a final set of experiments, we addressed the effect of Ni loading (2.6–10.4 wt% Ni) on the catalytic performance of Ni/CNFs pre-reduced at 773 K. Values of the actual Ni loading as measured with ICP-AES are listed in Table 4. Up to 10.4 wt% Ni, the metal loading barely affects the dispersion, and thus, the size distribution of the Ni particles. NH_3-TPD spectra and N_2 physisorption data closely resemble those of the Ni/CNFs reduced at 773 K described above and are therefore not shown. The acid densities, listed in Table 4, are almost insensitive to Ni loading, which enables a straightforward study of the metal function.

From the results given in Table 4, for up to 7.5 wt% Ni, the hexitol yield increases with increasing Ni loading. While in the case of 2.6 and 3.8 wt% Ni, relatively low yields of sorbitol and mannitol were detected, higher Ni loadings shift the product spectrum towards enhanced hexitol yields. At low Ni loadings, the poor selectivities can be tentatively explained by the acid and metal functions being out of balance, leading to a loss of glucose through thermal and acid-catalyzed degradation reactions.[10] Indeed, up to 2% glucose formation was evidenced in the product mixture sampled at short reaction times. In contrast, at Ni loadings higher than 7.5 wt%, several hydrogenolysis reactions of the C–C bonds in sorbitol become increasingly important and complicate the overall chemistry. To address this issue, results from a comparison of sorbitol stability after 24 h reaction time are given in Table 5, taking three Ni/CNFs with 2.6, 6.5, and 10.4 wt% Ni as representative catalysts. The results indicate a reduced sorbitol stability in the presence of 10.4 wt% Ni/CNFs, yielding a higher fraction of C_2–C_5 molecules. Erythritol, 1,2-butanediol, glycerol, 1,2-propanediol, and ethylene glycol were the predominant hydrogenolysis products irrespective of the Ni loading. Collecting all arguments

Table 4. Effect of the Ni loading on the properties of Ni/CNFs,[a] the conversion of cellulose, and product yields.[b]

Entry	Ni loading [wt%]	Acid density [mmol $g_{cat.}^{-1}$]	Ni dispersion [wt%]	Ni surface atoms [μmol $g_{cat.}^{-1}$]	Conversion [%]	Yield [%] hexitols	sorbitol	C_2–C_5 prod.
1	2.6	0.03	1.8	8.1	91.1	48.5	39.8	21.2
2	3.8	0.02	1.9	12.6	94.9	57.9	47.6	21.8
3	5.2	0.02	1.9	17.0	93.1	68.6	58.4	18.7
4	6.5	0.02	1.9	21.4	95.6	69.4	59.6	20.2
5	7.5	0.02	2.1	26.9	92.6	75.6	64.0	19.0
6	9.1	0.02	1.9	29.1	94.4	66.3	55.9	27.8
7	10.4	0.02	1.7	30.8	93.4	63.9	52.7	29.0

[a] Prepared by oxidation (twice in HNO_3 for 1 h), incipient wetness impregnation with varying concentrations of the Ni precursor ($[Ni^{2+}]$ = 0.01–0.05 g mL^{-1}), and reduction at 773 K. [b] Reaction conditions: ball-milled Avicel cellulose (1 g), Ni/CNFs (0.5 g), water (50 mL), 6 MPa initial H_2 pressure at RT, 463 K, 24 h.

 © 2012 Wiley-VCH Verlag GmbH & Co. KGaA, Weinheim

Table 5. Sorbitol conversion on Ni/CNF catalysts.[a]

Entry	Ni loading [wt%]	Sorbitol left in solution [%]	Mannitol yield [%]	C_2–C_5 product yield [%]
1	2.6	69.4	7.2	15.4
2	6.5	44.3	13.0	29.2
3	10.4	30.6	11.0	37.5

[a] Reaction conditions: sorbitol (1 g), Ni/CNF catalyst (0.5 g), water (50 mL), 6 MPa initial H_2 pressure at RT, 463 K, 24 h.

shows that an optimally balanced Ni loading is crucial for the selective conversion of cellulose because an excessive Ni loading favors C–C bond cleavage and inhibits hydrogenation.

As an addendum to the study of cellulose conversion, we also evaluated the use of Ni/CNFs for direct catalytic hydrogenation of glucose, using a pseudo-first-order kinetic approximation to probe the effect of Ni loading on the hydrogenation rate, as successfully applied in earlier work.[54] Batch experiments were performed at 398 K and 6 MPa H_2 pressure to avoid glucose caramelization. This is not an issue when starting from cellulose as a substrate, provided that, once small concentrations are formed by acid-catalyzed hydrolysis, glucose is rapidly hydrogenated.[1a] For the reactions shown in Figure 8, the Ni/CNF catalysts show a consistently high selectivity to sorbitol. For example, in case of the 10.4 wt% Ni/CNF catalyst, the yields of sorbitol reach values up to 96%.

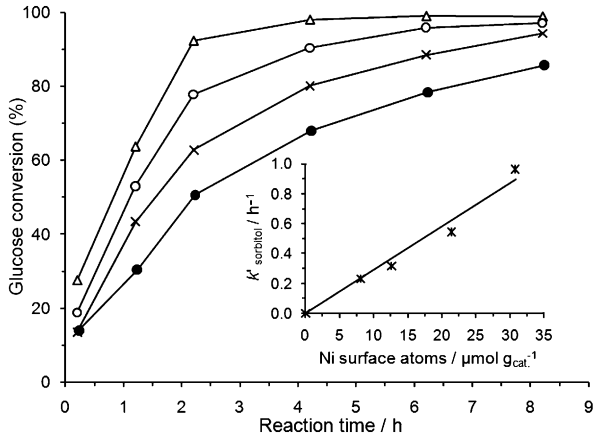

Figure 8. Effect of Ni loading on the catalytic hydrogenation of glucose to sorbitol at 398 K; ● 2.6, × 3.8, ○ 7.5, △ 10.4 wt% Ni. Reaction conditions: glucose (1 g), Ni/CNF catalyst (0.5 g), water (50 mL), 6 MPa initial H_2 pressure at RT, 398 K, 8 h. The inset shows the pseudo-first-order reaction rate versus the amount of Ni surface atoms for each Ni/CNF catalyst.

The product mixture also contained small amounts of gluconic acid (1.3%), which is a side product formed by the Cannizzaro reaction of glucose.[55] From the Arrhenius plot extracted from the pseudo-first-order reaction rates in the temperature range of 378–398 K, an apparent activation energy of about 52 kJ mol^{-1} was obtained. This value is appreciably higher than the activation energy of H_2 diffusion in liquids (12–21 kJ mol^{-1}), indicating that the catalytic hydrogenation experiments were performed in the kinetic regime.[54,56] As shown in the inset in Figure 8, a nearly linear correlation is observed between the pseudo-first-order reaction rates constants for sorbitol formation and the amount of Ni surface atoms of the Ni/CNFs. These results clearly establish a linear dependence of the hydrogenation activity of the Ni/CNFs on the availability of surface metal sites.

Evaluation of the catalyst acid/metal balance

The experimental data set thus far obtained has been used to rationalize the acid/metal balance requirements of the Ni/CNFs for hydrolytic hydrogenation of cellulose to hexitols. Inspiration for the applied methodology was found in related literature available on the evaluation of bifunctional catalysts for hydrocracking of alkanes.[57] Taking the characterization results reported in Tables 1 and 4, the ratio of the acid density to the number of Ni surface atoms (n_A/n_{Ni}) was used to monitor the balance between the hydrogenation and the acid functions. The applicability of this parameter can be assessed by studying Figure 9, in which the n_A/n_{Ni} values and the corresponding hexitol yields are presented.

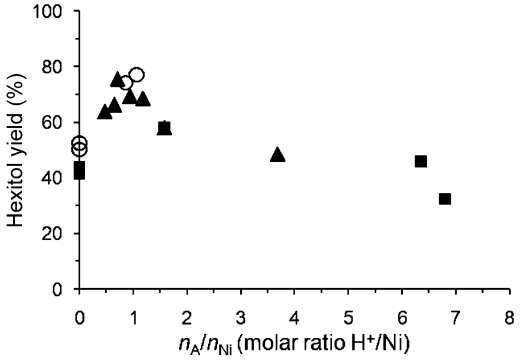

Figure 9. Relationship between the n_A/n_{Ni} ratio and the observed hexitol yields for the Ni/CNF catalysts discussed: effect of nature of oxidation agent for support treatment (○), effect of catalyst reduction temperature (■), and effect of Ni loading (▲).

Considering the inevitable experimental error in this type of reactions, the observed relationship appears to be relatively good. The reduced hexitol yields (42–53%) generated for non-acidic Ni/CNFs ($n_A/n_{Ni}=0$) suggest the need for acid sites on the CNF surface in the catalytic depolymerization of cellulose and other subsequent hydrolysis reactions. When the acid density is high enough to establish a proper balance between the two catalytic functions ($0.7 < n_A/n_{Ni} < 1.1$), the hexitol yield reaches a maximum of nearly 80%. For lower values, a further increase in the amount of Ni surface atoms renders the sugar alcohols more susceptible to C–C bond hydrogenolysis; hence, lowering the C_6 product selectivity. For increasingly higher values of this ratio, it is more likely that glucose is subjected to another acid-catalyzed degradation reaction rather than being hydrogenated to hexitols.

 © 2012 Wiley-VCH Verlag GmbH & Co. KGaA, Weinheim

Conclusions

A series of well-characterized Ni/CNFs were tested for the hydrolytic hydrogenation of cellulose to C_6 sugar alcohols. Variations in the nature of the oxidation agent for support treatment (HNO_3 vs. 1:1 mixtures of HNO_3/H_2SO_4), the Ni activation procedure (different reduction temperatures), and Ni loading enabled us to tune the dispersion of the Ni particles, as well as the number of oxygen-containing surface groups. The catalytic results presented herein not only give insight into the optimal preparation conditions of bifunctional Ni/CNFs for cellulose to hexitol conversion, but also advance a diagnostic tool to evaluate the balance between the hydrogenation and the acid functions. In the investigated range of conditions, the 7.5 wt% Ni/CNFs with a relatively high amount of Ni surface atoms (26.9 $\mu mol\, g_{cat.}^{-1}$) and low density of Brønsted acid sites (0.02 $mmol_{H^+}\, g^{-1}$), prepared by an oxidative activation of fishbone-type CNFs in HNO_3, incipient wetness impregnation, and a reduction up to 773 K under H_2, showed the highest hexitol yields of up to 76% at a cellulose conversion of 93%.

Experimental Section

Catalyst preparation: For the catalytic growth of CNFs, 20 wt% Ni/γ-Al_2O_3 was prepared by wet impregnation of alumina (Puralox, 155 $m^2\, g^{-1}$) with an aqueous solution of nickel nitrate ($[Ni^{2+}] =$ 0.17–0.95 $mmol\, L^{-1}$). After drying at 373 K, the catalyst precursor was calcined for 5 h in static air at 873 K (heating rate 5 $K\, min^{-1}$). Prior to fiber growth, the Ni-catalyst precursor (1 g) was reduced for 1 h under a flow of H_2 (50 $mL\, min^{-1}$) at 873 K (heating rate 5 $K\, min^{-1}$). Next, the CNFs were grown by CVD of CH_4 (80 $mL\, min^{-1}$) at 873 K for 3.5 h. Typically, a CNF yield of 6 g was obtained. A more detailed description of CNF growth can be found elsewhere.[22] For a typical activation of the CNFs by surface oxidation and removal of Ni, a suspension of CNFs (6 g) in HNO_3 (120 mL; 65%) was heated at 383 K under vigorous stirring. After 1 h, the oxidized CNFs were filtered, washed with distilled water, and dried overnight at 373 K. Ni was deposited on the oxidized CNFs by using the incipient wetness impregnation technique. Briefly, the desired amount of $Ni(NO_3)_2{\cdot}6H_2O$ was dissolved in distilled water (2 mL) and added dropwise to the CNFs (1 g). Next, the samples were dried at 333 K for 12 h, heated under N_2 to 773 K (heating rate 5 $K\, min^{-1}$), and reduced for 1 h under a flow of H_2 (100 $mL\, min^{-1}$).

Catalyst characterization: Brunauer–Emmett–Teller specific surface areas (S_{BET}) and pore volumes of the catalysts were calculated from N_2 physisorption data obtained at 77 K by using a Micromeritics Tristar 3000 apparatus. Prior to the physisorption experiments, the samples were evacuated at 473 K for at least 12 h. Quantitative elemental analysis of the Ni loading was performed by ICP-AES using a Jobin–Yvon Ultima spectrometer. The acidic properties of the catalysts were determined by NH_3-TPD and acid–base titrations. For NH_3-TPD experiments, the activated Ni/CNF samples (100 mg) were placed in a quartz reactor and covered with quartz beads. Outlet gases were analyzed with a mass spectrometer equipped with a quadruple mass filter (Balzers QMC 200). Samples were first dehydrated under pure He at 773 K to obtain a flat water signal (*m/z* 17 and 18). Then, samples were cooled to RT under a flow of He. NH_3 adsorption was performed by passing a flow of 5% NH_3 in He through the sample bed. Excess NH_3 was evacuated at RT by passing a flow of pure He until a flat NH_3 signal (*m/z* 15, 16 and 17) was obtained. Desorption of the adsorbed NH_3 was performed by increasing the temperature to 873 K at 10 $K\, min^{-1}$. The signal corresponding to *m/z* 16, assigned to NH_3, was used for the analysis of the NH_3-TPD curves. Standard acid–base titration was performed by suspending CNFs (100 mg) in a 0.1 M aqueous solution of KCl (25 mL). The mixture was vigorously stirred overnight. Prior to measurement, the mixture was degassed under Ar for at least 1 h. While stirring, the amount of acid sites was determined by dropwise addition of an aqueous solution containing 0.01 M NaOH and 0.1 M KCl using a Metrohm 808 Titrando autotitrator & 801 stirrer.

The amount of Ni surface atoms was determined by using pulsed CO titration experiments. Approximately 50 mg of the catalyst sample was placed into a tubular reactor and pretreated in a flow of H_2 (20 $mL\, min^{-1}$) for 1 h at 773 K (heating rate 5 $K\, min^{-1}$). Afterwards, the sample was purged with He and cooled to RT. Pulses of 5 μL of pure CO were added through a calibrated loop to a He flow of 20 $mL\, min^{-1}$ at an interval of 2 min. The CO concentration in the outlet stream was followed by ion monitoring at *m/z* 28 with a Pfeiffer Omnistar quadrupole mass spectrometer. The integration of the resultant CO peak areas was performed by using Origin Pro 8 software (OriginLab). H_2-TPR profiles were obtained in the same apparatus by using MS detection under the following conditions: sample weight 100 mg, heating rate 10 $K\, min^{-1}$, flow rate 12 $mL\, min^{-1}$, and 5 vol% H_2 in N_2. Prior to reduction, the samples were dried at 373 K. For temperature-programmed decomposition experiments, about 50 mg of the sample was placed in the sample holder and degassed under a flow of He (20 $mL\, min^{-1}$). The temperature was increased from 298 to 1373 K (heating rate 10 $K\, min^{-1}$); and the partial pressures of CO and CO_2 were recorded by using a mass spectrometer.

XPS was performed on a SSX 100/206 photoelectron spectrometer from Surface Science Instruments (USA) equipped with a monochromated microfocused Al X-ray source (powered at 20 mA and 10 kV). The sample powder pressed in small stainless-steel troughs of 4 mm diameter was placed on an insulating ceramic insulator carousel. The pressure in the analysis chamber was around 10^{-6} Pa. The angle between the surface normal and the axis of the analyzer lens was 55°. The analyzed area was approximately 1.4 mm^2, and the pass energy was set at 150 eV. In these conditions, the full width at half maximum of the Au $4f_{7/2}$ peak of a clean gold standard sample was about 1.6 eV. A flood gun set at 8 eV and a Ni grid placed 3 mm above the sample surface were used for charge stabilization. Data treatment was performed by using the CasaXPS program (Casa Software). Some spectra were decomposed with the least-squares fitting routine provided by the software with a Gaussian/Lorentzian (85/15) product function and after subtraction of a nonlinear baseline.

Catalyst testing: The conversion of cellulose was studied in batch mode in a 100 mL Parr autoclave equipped with a mechanical stirrer, a liquid sampling tube, gas inlet and outlet tubes, a thermocouple, a rupture disc, and an electric heating jacket. The autoclave was loaded with cellulose (1 g) and the reduced catalyst (0.5 g) in distilled water (50 mL). After flushing the reaction mixture with N_2, 6 MPa of H_2 was added to the autoclave and the temperature was raised to 463 K. To operate in the kinetically controlled regime, the stirrer speed was set at 700 rpm. The short heating time (15 min) and the accurate temperature control ensured stable conditions during the reaction. Experiments with glucose were performed at 398 K and a H_2 pressure of 6 MPa added at RT.

Product analysis: Samples of the reaction mixture (ca. 1 mL) were withdrawn periodically, centrifuged, filtered over a 0.45 μm PTFE

 © 2012 Wiley-VCH Verlag GmbH & Co. KGaA, Weinheim

filter, and analyzed by HPLC (Agilent 1200 Series, Varian Metacarb 67C column (300×6.5 mm), mobile phase: 0.5 mL min^{-1} of water), equipped with a refractive index detector. The product yield was calculated as follows: yield (%) = (weight of polyol)/(weight of cellulose charged in reactor). Conversions of cellulose were determined by TOC analysis of the liquid phase, as reported earlier.[22] Water-soluble cello-oligomers were analyzed by HPAEC-PAD performed on a Dionex ICS-3000 chromatography system (Dionex Corporation, Sunnyvale, CA, USA). The product mixture was diluted (1:200 in water) and filtered (Millex-GP, 0.22 μm, polyethersulfone; Millipore, Carrigtwohill, Ireland) before injection on a CarboPac PA-100 anion-exchange column (250×4 mm). The mobile phase was composed of A (H_2O), B (200 mM NaOH), and C (400 mM NaOAc in 100 mM NaOH). Water-soluble cello-oligomers were separated by running a linear gradient of A/B/C changing from 50:50:0 to 12.5:12.5:75 within 25 min at a flow rate of 1 mL min^{-1}, followed by 25–30 min elution with a 100% C solution. The column temperature was maintained at 303 K.

Acknowledgements

This work was supported by the IAP-VI program "Supramolecular Chemistry and Catalysis" of the Belgian Federal government. Long-term structural funding was provided by the Methusalem Grant of the Flemish government. S.V.d.V., W.S., M.D., and E.D. acknowledge the Research Foundation - Flanders (FWO) for doctoral and postdoctoral fellowships. J.G. is grateful to the Institute for the Promotion of Innovation through Science and Technology in Flanders (IWT-Vlaanderen) for a doctoral fellowship. J.W.S. thanks the Flemish Hercules Stichting for its support in HER/08/25. We acknowledge S. Mannaerts for ICP-AES analysis, G. Vanbutsele for N_2 physisorption analysis, and W. Vermandel for help with H_2-TPR and CO chemisorption measurements.

Keywords: carbohydrates · cellulose · heterogeneous catalysis · nanostructures · nickel

[1] a) S. Van de Vyver, J. Geboers, P. A. Jacobs, B. F. Sels, *ChemCatChem* **2011**, *3*, 82–94; b) J. A. Geboers, S. Van de Vyver, R. Ooms, B. Op de Beeck, P. A. Jacobs, B. F. Sels, *Catal. Sci. Technol.* **2011**, *1*, 714–726; c) P. Gallezot, *Chem. Soc. Rev.* **2012**, *41*, 1538–1558; d) M. Rose, R. Palkovits, *ChemSusChem* **2012**, *5*, 167–176; e) J.-P. Lange, E. van der Heide, J. van Buijtenen, R. Price, *ChemSusChem* **2012**, *5*, 150–166; f) Y. Román-Leshkov, M. E. Davis, *ACS Catal.* **2011**, *1*, 1566–1580; g) P. F. Yang, H. Kobayashi, A. Fukuoka, *Chin. J. Catal.* **2011**, *32*, 716–722; h) R. Palkovits, *Chem. Ing. Tech.* **2011**, *83*, 411–419; i) A. Cabiac, E. Guillon, F. Chambon, C. Pinel, F. Rataboul, N. Essayem, *Appl. Catal. A: Gen.* **2011**, *402*, 1–10; j) C.-H. Zhou, X. Xia, C.-X. Lin, D.-S. Tong, J. Beltramini, *Chem. Soc. Rev.* **2011**, *40*, 5588–5617; k) H. Kobayashi, T. Komanoya, S. K. Guha, K. Hara, A. Fukuoka, *Appl. Catal. A: Gen.* **2011**, *409–410*, 13–20; l) J. C. Serrano-Ruiz, J. A. Dumesic, *Energy Environ. Sci.* **2011**, *4*, 83–99; m) J. J. Verendel, T. L. Church, P. G. Andersson, *Synthesis* **2011**, *11*, 1649–1677; n) G. Centi, P. Lanzafame, S. Perathoner, *Catal. Today* **2011**, *167*, 14–30; o) M. J. Climent, A. Corma, S. Iborra, *Green Chem.* **2011**, *13*, 520–540; p) J. J. Bozell, G. R. Petersen, *Green Chem.* **2010**, *12*, 539–554; q) M. Rose, R. Palkovits, *Macromol. Rapid Commun.* **2011**, *32*, 1299–1311; r) K.-i. Shimizu, A. Satsuma, *Energy Environ. Sci.* **2011**, *4*, 3140–3153; s) D. M. Alonso, J. Q. Bond, J. A. Dumesic, *Green Chem.* **2010**, *12*, 1493–1513; t) R. Rinaldi, F. Schüth, *Energy Environ. Sci.* **2009**, *2*, 610–626; u) R. Rinaldi, F. Schüth, *ChemSusChem* **2009**, *2*, 1096–1107; v) A. Fukuoka, P. L. Dhepe, *Chem. Rec.* **2009**, *9*, 224–235; w) P. L. Dhepe, A. Fukuoka, *ChemSusChem* **2008**, *1*, 969–975; x) J. N. Chheda, G. W. Huber, J. A. Dumesic, *Angew. Chem.* **2007**, *119*, 7298–7318; *Angew. Chem. Int. Ed.* **2007**, *46*, 7164–7183; y) B. Kamm, *Angew. Chem.* **2007**, *119*, 5146–5149; *Angew. Chem. Int. Ed.* **2007**, *46*, 5056–5058; z) P. Gallezot, *Green Chem.* **2007**, *9*, 295–302; aa) A. M. Ruppert, K. Weinberg, R. Palkovits, *Angew. Chem.* **2012**, *124*, 2614–2654; *Angew. Chem. Int. Ed.* **2012**, *51*, 2564–2601; ab) S. Van de Vyver, J. Geboers, S. Helsen, F. Yu, J. Thomas, M. Smet, W. Dehaen, B. F. Sels, *Chem. Commun.* **2012**, *48*, 3497–3499; ac) H. Kobayashi, H. Ohta, A. Fukuoka, *Catal. Sci. Technol.* **2012**, *2*, 869–883; ad) D. Reyes-Luyanda, J. Flores-Cruz, P. J. Morales-Pérez, L. G. Encarnación-Gòmez, F. Shi, P. M. Voyles, N. Cardona-Martínez, *Top. Catal.* **2012**, *55*, 148–161; ae) R. Weingarten, W. C. Conner, G. W. Huber, *Energy Environ. Sci.* **2012**, *5*, 7559–7574.

[2] a) A. A. Balandin, N. A. Vasunina, S. V. Chepigo, G. S. Barysheva, *Dokl. Akad. Nauk Sssr* **1959**, *128*, 941–944; b) V. I. Scharkow, *Chem. Ingr. Tech.* **1963**, *35*, 494–497; c) V. I. Sharkov, *Angew. Chem.* **1963**, *75*, 805–812; *Angew. Chem. Int. Ed. Engl.* **1963**, *2*, 405–409.

[3] a) A. Fukuoka, P. L. Dhepe, *Angew. Chem.* **2006**, *118*, 5285–5287; *Angew. Chem. Int. Ed.* **2006**, *45*, 5161–5163; b) P. Dhepe, A. Fukuoka, *Catal. Surv. Asia* **2007**, *11*, 186–191; c) V. Jollet, F. Chambon, F. Rataboul, A. Cabiac, C. Pinel, E. Guillon, N. Essayem, *Green Chem.* **2009**, *11*, 2052–2060.

[4] H. Kobayashi, Y. Ito, T. Komanoya, Y. Hosaka, P. L. Dhepe, K. Kasai, K. Hara, A. Fukuoka, *Green Chem.* **2011**, *13*, 326–333.

[5] S. You, I. Baek, Y. Kim, K.-E. Jeong, H.-J. Chae, T.-W. Kim, C.-U. Kim, S.-Y. Jeong, T. Kim, Y.-M. Chung, S.-H. Oh, E. Park, *Korean J. Chem. Eng.* **2011**, *28*, 744–750.

[6] M. Käldström, N. Kumar, D. Y. Murzin, *Catal. Today* **2011**, *167*, 91–95; b) M. Käldström, N. Kumar, M. Tenho, M. V. Mokeev, Y. E. Moskalenko, D. Y. Murzin, *ACS Catal.* **2012**, *2*, 1381–1393.

[7] a) C. Luo, S. Wang, H. C. Liu, *Angew. Chem.* **2007**, *119*, 7780–7783; *Angew. Chem. Int. Ed.* **2007**, *46*, 7636–7639; b) H. Kobayashi, H. Matsuhashi, T. Komanoya, K. Hara, A. Fukuoka, *Chem. Commun.* **2011**, *47*, 2366–2368; c) S. K. Guha, H. Kobayashi, K. Hara, H. Kikuchi, T. Aritsuka, A. Fukuoka, *Catal. Commun.* **2011**, *12*, 980–983.

[8] a) J. Geboers, S. Van de Vyver, K. Carpentier, K. de Blochouse, P. Jacobs, B. Sels, *Chem. Commun.* **2010**, *46*, 3577–3579; b) R. Palkovits, K. Tajvidi, A. M. Ruppert, J. Procelewska, *Chem. Commun.* **2011**, *47*, 576–578; c) J. Geboers, S. Van de Vyver, K. Carpentier, P. Jacobs, B. Sels, *Green Chem.* **2011**, *13*, 2167–2174.

[9] Y. Ogasawara, S. Itagaki, K. Yamaguchi, N. Mizuno, *ChemSusChem* **2011**, *4*, 519–525.

[10] J. Geboers, S. Van de Vyver, K. Carpentier, P. Jacobs, B. Sels, *Chem. Commun.* **2011**, *47*, 5590–5592.

[11] a) W. Deng, X. Tan, W. Fang, Q. Zhang, Y. Wang, *Catal. Lett.* **2009**, *133*, 167–174; b) W. Deng, M. Liu, X. Tan, Q. Zhang, Y. Wang, *J. Catal.* **2010**, *271*, 22–32; c) H. Wang, L. Zhu, S. Peng, F. Peng, H. Yu, J. Yang, *Renewable Energy* **2012**, *37*, 192–196.

[12] M. Liu, W. Deng, Q. Zhang, Y. Wang, Y. Wang, *Chem. Commun.* **2011**, *47*, 9717–9719.

[13] I. A. Ignatyev, C. Van Doorslaer, P. G. N. Mertens, K. Binnemans, D. E. De Vos, *ChemSusChem* **2010**, *3*, 91–96.

[14] J. Pang, A. Wang, M. Zheng, Y. Zhang, Y. Huang, X. Chen, T. Zhang, *Green Chem.* **2012**, *14*, 614–617.

[15] G. Liang, C. Wu, L. He, J. Ming, H. Cheng, L. Zhuo, F. Zhao, *Green Chem.* **2011**, *13*, 839–842.

[16] R. Palkovits, K. Tajvidi, J. Procelewska, R. Rinaldi, A. Ruppert, *Green Chem.* **2010**, *12*, 972–978.

[17] a) N. Ji, T. Zhang, M. Zheng, A. Wang, H. Wang, X. Wang, J. G. Chen, *Angew. Chem.* **2008**, *120*, 8638–8641; *Angew. Chem. Int. Ed.* **2008**, *47*, 8510–8513; b) N. Ji, T. Zhang, M. Y. Zheng, A. Q. Wang, H. Wang, X. D. Wang, Y. Y. Shu, A. L. Stottlemyer, J. G. G. Chen, *Catal. Today* **2009**, *147*, 77–85; c) C. Li, M. Zheng, A. Wang, T. Zhang, *Energy Environ. Sci.* **2012**, *5*, 6383–6390; d) N. Ji, M. Zheng, A. Wang, T. Zhang, J. G. Chen, *ChemSusChem* **2012**, *5*, 939–944.

[18] M. Y. Zheng, A. Q. Wang, N. Ji, J. F. Pang, X. D. Wang, T. Zhang, *ChemSusChem* **2010**, *3*, 63–66.

[19] Y. Zhang, A. Wang, T. Zhang, *Chem. Commun.* **2010**, *46*, 862–864.

[20] Y. Liu, C. Luo, H. Liu, *Angew. Chem.* **2012**, *124*, 3303–3307; *Angew. Chem. Int. Ed.* **2012**, *51*, 3249–3253.

[21] L.-N. Ding, A.-Q. Wang, M.-Y. Zheng, T. Zhang, *ChemSusChem* **2010**, *3*, 818–821.

 © 2012 Wiley-VCH Verlag GmbH & Co. KGaA, Weinheim

[22] S. Van de Vyver, J. Geboers, M. Dusselier, H. Schepers, T. Vosch, L. A. Zhang, G. Van Tendeloo, P. A. Jacobs, B. F. Sels, *ChemSusChem* **2010**, *3*, 698 – 701.
[23] a) M. S. Hoogenraad, R. A. G. M. M. van Leeuwarden, G. J. B. van Breda Vriesman, A. Broersma, A. J. van Dillen, J. W. Geus, *Stud. Surf. Sci. Catal.* **1995**, *91*, 263 – 271; b) J. K. Chinthaginjala, K. Seshan, L. Lefferts, *Ind. Eng. Chem. Res.* **2007**, *46*, 3968 – 3978.
[24] a) K. P. De Jong, J. W. Geus, *Catal. Rev. Sci. Eng.* **2000**, *42*, 481 – 510; b) N. M. Rodriguez, A. Chambers, R. T. K. Baker, *Langmuir* **1995**, *11*, 3862 – 3866.
[25] S. K. Shaikhutdinov, L. B. Avdeeva, B. N. Novgorodov, V. I. Zaikovskii, D. I. Kochubey, *Catal. Lett.* **1997**, *47*, 35 – 42.
[26] P. Liu, H. Xie, S. Tan, K. You, N. Wang, H. a. Luo, *React. Kinet. Catal. Lett.* **2009**, *97*, 101 – 108.
[27] F. Salman, C. Park, R. T. K. Baker, *Catal. Today* **1999**, *53*, 385 – 394.
[28] A. Nieto-Márquez, V. Jiménez, A. M. Raboso, S. Gil, A. Romero, J. L. Valverde, *Appl. Catal. A: Gen.* **2011**, *393*, 78 – 87.
[29] A. Nieto-Márquez, S. Gil, A. Romero, J. L. Valverde, S. Gomez-Quero, M. A. Keane, *Appl. Catal. A: Gen.* **2009**, *363*, 188 – 198.
[30] a) C. Park, R. T. K. Baker, *J. Phys. Chem. B* **1998**, *102*, 5168 – 5177; b) C. Park, R. T. K. Baker, *J. Phys. Chem. B* **1999**, *103*, 2453 – 2459.
[31] A. Chambers, T. Nemes, N. M. Rodriguez, R. T. K. Baker, *J. Phys. Chem. B* **1998**, *102*, 2251 – 2258.
[32] a) P. Serp, M. Corrias, P. Kalck, *Appl. Catal. A: Gen.* **2003**, *253*, 337 – 358; b) J. H. Bitter, K. P. de Jong in *Carbon Materials for Catalysis* (Eds.: P. Serp, J. L. Figueiredo), Wiley, New York **2008**, pp. 157 – 176.
[33] E. Ochoa-Fernández, D. Chen, Z. Yu, B. Tøtdal, M. Rønning, A. Holmen, *Catal. Today* **2005**, *102 – 103*, 45 – 49.
[34] M. S. Hoogenraad, Ph.D. Thesis, Utrecht University (The Netherlands), **1995**.
[35] L. M. Ang, T. S. A. Hor, G. Q. Xu, C. H. Tung, S. P. Zhao, J. L. S. Wang, *Carbon* **2000**, *38*, 363 – 372.
[36] a) M. K. van der Lee, J. van Dillen, J. H. Bitter, K. P. de Jong, *J. Am. Chem. Soc.* **2005**, *127*, 13573 – 13582; b) J. H. Bitter, M. K. van der Lee, A. G. T. Slotboom, A. J. van Dillen, K. P. de Jong, *Catal. Lett.* **2003**, *89*, 139 – 142.
[37] F. Rodríguez-reinoso, *Carbon* **1998**, *36*, 159 – 175.
[38] a) B.-W. Chun, C. Randall Davis, Q. He, R. R. Gustafson, *Carbon* **1992**, *30*, 177 – 187; b) T. G. Ros, A. J. van Dillen, J. W. Geus, D. C. Koningsberger, *Chem. Eur. J.* **2002**, *8*, 1151 – 1162.
[39] R. Rinaldi, A. d. M. Porcari, T. C. R. Rocha, W. H. Cassinelli, R. U. Ribeiro, J. M. C. Bueno, D. Zanchet, *J. Mol. Catal. A: Chem.* **2009**, *301*, 11 – 17.
[40] M. L. Toebes, J. M. P. van Heeswijk, J. H. Bitter, A. Jos van Dillen, K. P. de Jong, *Carbon* **2004**, *42*, 307 – 315.
[41] A. Rinaldi, N. Abdullah, M. Ali, A. Furche, S. B. A. Hamid, D. S. Su, R. Schlögl, *Carbon* **2009**, *47*, 3023 – 3033.
[42] M. K. van der Lee, Ph.D. Thesis, Utrecht University (The Netherlands), **2005**.
[43] a) S. Van de Vyver, L. Peng, J. Geboers, H. Schepers, F. de Clippel, C. J. Gommes, B. Goderis, P. A. Jacobs, B. F. Sels, *Green Chem.* **2010**, *12*, 1560 – 1563; b) S. Van de Vyver, J. Thomas, J. Geboers, S. Keyzer, M. Smet, W. Dehaen, P. A. Jacobs, B. F. Sels, *Energy Environ. Sci.* **2011**, *4*, 3601 – 3610.
[44] N. Li, G. W. Huber, *J. Catal.* **2010**, *270*, 48 – 59.
[45] a) R. Rinaldi, N. Meine, J. vom Stein, R. Palkovits, F. Schüth, *ChemSusChem* **2010**, *3*, 266 – 276; b) R. Rinaldi, P. Engel, J. Büchs, A. C. Spiess, F. Schüth, *ChemSusChem* **2010**, *3*, 1151 – 1153; c) R. Rinaldi, R. Palkovits, F. Schüth, *Angew. Chem.* **2008**, *120*, 8167 – 8170; *Angew. Chem. Int. Ed.* **2008**, *47*, 8047 – 8050.
[46] a) H. G. M. Edwards, V. Fawcett, *J. Mol. Struct.* **1994**, *326*, 131 – 143; b) N. Hung, N. Tuong, E. Rakov, *Inorg. Mater.* **2010**, *46*, 1077 – 1083.
[47] J.-H. Zhou, Z.-J. Sui, J. Zhu, P. Li, D. Chen, Y.-C. Dai, W.-K. Yuan, *Carbon* **2007**, *45*, 785 – 796.
[48] L. Calvillo, M. Gangeri, S. Perathoner, G. Centi, R. Moliner, M. J. Lázaro, *J. Power Sources* **2009**, *192*, 144 – 150.
[49] a) R. T. K. Baker, *J. Catal.* **1982**, *78*, 473 – 476; b) R. T. K. Baker, P. S. Harris, R. B. Thomas, *Surf. Sci.* **1974**, *46*, 311 – 316; c) R. T. K. Baker, *Catal. Rev. Sci. Eng.* **1979**, *19*, 161 – 209.
[50] a) A. E. Aksoylu, M. M. A. Freitas, J. L. Figueiredo, *Appl. Catal. A: Gen.* **2000**, *192*, 29 – 42; b) J. L. Figueiredo, M. F. R. Pereira, M. M. A. Freitas, J. J. M. Órfão, *Carbon* **1999**, *37*, 1379 – 1389; c) F. de Clippel, A. Harkiolakis, T. Vosch, X. Ke, L. Giebeler, S. Oswald, K. Houthoofd, J. Jammaer, G. Van Tendeloo, J. A. Martens, P. A. Jacobs, G. V. Baron, B. F. Sels, J. F. M. Denayer, *Microporous Mesoporous Mater.* **2011**, *144*, 120 – 133.
[51] M. L. Toebes, M. K. van der Lee, L. M. Tang, M. H. H. in 't Veld, J. H. Bitter, A. J. van Dillen, K. P. de Jong, *J. Phys. Chem. B* **2004**, *108*, 11611 – 11619.
[52] Q. L. Zhuang, T. Kyotani, A. Tomita, *Carbon* **1994**, *32*, 539 – 540.
[53] A. P. Grosvenor, M. C. Biesinger, R. S. C. Smart, N. S. McIntyre, *Surf. Sci.* **2006**, *600*, 1771 – 1779.
[54] E. Crezee, B. W. Hoffer, R. J. Berger, M. Makkee, F. Kapteijn, J. A. Moulijn, *Appl. Catal. A: Gen.* **2003**, *251*, 1 – 17.
[55] P. Gallezot, P. J. Cerino, B. Blanc, G. Flèche, P. Fuertes, *J. Catal.* **1994**, *146*, 93 – 102.
[56] N. Déchamp, A. Gamez, A. Perrard, P. Gallezot, *Catal. Today* **1995**, *24*, 29 – 34.
[57] a) T. F. Degnan, C. R. Kennedy, *AIChE J.* **1993**, *39*, 607 – 614; b) F. Alvarez, F. R. Ribeiro, G. Perot, C. Thomazeau, M. Guisnet, *J. Catal.* **1996**, *162*, 179 – 189; c) J. W. Thybaut, C. S. Laxmi Narasimhan, J. F. Denayer, G. V. Baron, P. A. Jacobs, J. A. Martens, G. B. Marin, *Ind. Eng. Chem. Res.* **2005**, *44*, 5159 – 5169; d) M. J. Girgis, Y. P. Tsao, *Ind. Eng. Chem. Res.* **1996**, *35*, 386 – 396.

Received: December 1, 2011
Published online on June 22, 2012

 © 2012 Wiley-VCH Verlag GmbH & Co. KGaA, Weinheim